

Experimental investigations for a postweld heat treatment on Ti-6Al-4V titanium welds with a defocused laser beam

J.D. Beguin¹, Y. Balcaen¹, J. Alexis¹, and E. Andrieu²

¹Université de Toulouse, LGP, ENIT/INPT, 47 Avenue d'Azereix, 65016 Tarbes, France

² Université de Toulouse, Institut CARNOT CIRIMAT, UPS/CNRS/INPT, ENSIACET, 4 allée Emile Monso, 31030 Toulouse, France

Corresponding author : Jean-denis Beguin, jean-denis.beguin@enit.fr.

Abstract

The purpose of this study is to apply a local heat treatment (LHT), in-situ, on the weld bead, using a defocused Yb: YAG laser beam on a continuous regime, in order to reduce residual stresses and decompose the brittle α' martensite, into a lamellae and fine β phase. Laser scan experiments were firstly performed on a commercially pure titanium grade 2, with a wide range of parameters, in order to provide a "heat treatment window" without titanium melting. After optimization of the processing parameters, to obtain a sufficient width and depth for the scanning zone, experiments have been performed on a β -treated, fully martensitic Ti-6Al-4V sheet. For each processing experiments, the decomposition of α' , was studied based on metallographic cross sections. A local heating with a minimum energy density at 700 J.cm^{-2} , has a sufficient effect to destabilize α' , while for an energy density at 1000 J.cm^{-2} , a diffusional transformation take place, with the formation of Widmanstätten microstructure. Finally, these optimized conditions were applied on a full penetration Ti-6Al-4V welds. The results of the LHT will be described in terms of the microstructural changes observed in the welded zone and hardness evolution.

1. Introduction

Laser welding is a rapid and accurate process to join thin components with complex geometry and minimal heat input. Nevertheless, High cooling rate in the fusion zone (FZ), induces high level of residual stresses, and a significant local microstructural change, with a very complex microstructure, varying from α' phase in the FZ, to a mixture of α and α' phase, in the heat affected zone (HAZ) of titanium alloys [1]. This microstructural change reduces the elongation at 5% approximately, with a similar or slightly higher tensile strength compare to the base metal (BM). These mechanical properties can be mainly attributed to the formation of a brittle martensite microstructure, for the Ti-6Al-4V alloy [2] [3]. As a consequence, post-weld heat treatments are generally applied to obtain an homogeneous microstructure in FZ, with α and β phase and a balanced tensile properties [4]. The aim of this work is to propose a LHT on the welds, using a defocused laser beam, by passing standard heat treatments, implying use of larges furnaces under protective atmosphere.

2. Material and experiments

Commercially pure titanium (CP ASTM grade 2) sheets (0.8 mm thick) and Ti-6Al-4V (ASTM grade 5) sheets (0.9 mm thick), were used as the base material. The microstructure of the base metal consists on a fine recrystallized α phase grains for the CP Ti and a classic annealed microstructure for the Ti-6Al-4V titanium alloy, composed of equiaxed α nodules surrounded by thin β phase.

A continuous Yb: YAG Trumph laser disk beam was used to realize welding and post-heat treatment. Welding was realized with the 100 μm core fiber and the 400 μm ring fiber. The Ti-6Al-4V plates were welded in a butt joint configuration. Before welding, titanium plates were mechanically polished with a P600 SiC paper, water rinsed and cleaned by acetone. A trailing shield was used to protect the top of the weld, in the welding configuration (Figure 1a) and a gas nozzle adjustable in height position, for the Local Heat Treatment (Figure 1b). To protect the back of the weld, a back shielding arrangement is incorporated into the fixture.

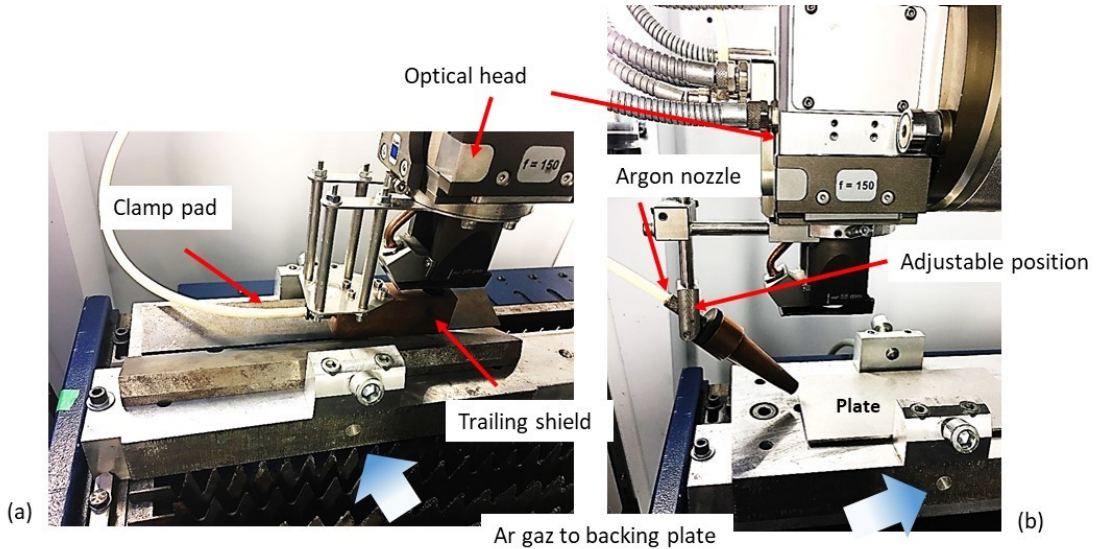


Figure 1: Experimental set-up (a) welding configuration, (b) Local Heat Treatment configuration

The microstructure of a Ti-6Al-4V weld (Figure 2), consists of fine acicular α' martensite in the Fusion Zone (FZ) and a mixture of α , β and α' phase in the Heat affected Zone (HAZ). To attain a fully martensitic microstructure on Ti-6Al-4V, a cooling rate higher than $410^\circ\text{C}\cdot\text{s}^{-1}$ is required [5].

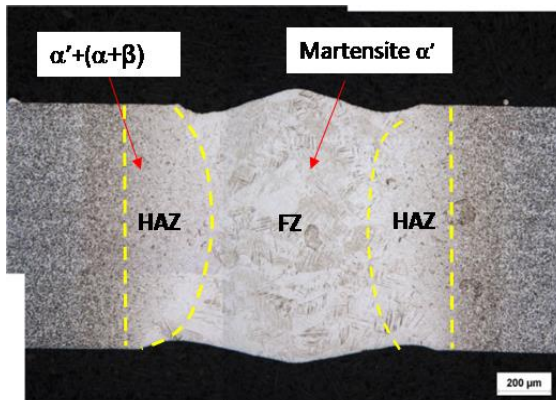


Figure 2: Typical microstructure of Ti-6Al-4V laser weld ($1500\text{ W}; 4,5\text{ m}\cdot\text{s}^{-1}$; spot size $370\ \mu\text{m}$ focused at $0,3\text{ mm}$ under the surface).

The measured welded-bead dimensions, in the weldability window [6], with the criterion of “full penetration”, are given in the table 1.

Table 1: Dimensions of Ti-6Al-4V welds in the weldability window for a full penetration.

fiber type	FZ width (mm)	HAZ width (mm)	FZ penetration (mm)
Core 100 μm	0,5 to 1,4	0,1 to 0,7	0,6 to 0,9
Ring core 400 μm	0,6 to 1,4	0,1 to 0,5	0,1 to 0,9

The first research task was to perform laser tracks on a CP grade 2 plate, using a defocused laser, to highlight a heat treatable region, without melting. The defocused laser mode was obtained by moving the optic head vertically, to adapt the size of the spot laser beam to the dimensions of the weld. The experience design implemented to achieve this objective is given in the table Table 2.

Table 2: Experimental parameters to determine the heat treatment with a temperature below the melting point.

Process parameters	Values	Responses (NF-LF06-395)
Power [W]	300-3000 (5 levels)	HAZ Width
Speed [m/min]	10-100 (8 levels)	HAZ penetration
Defocused distance (mm)	120-750 (5 levels)	Microstructure
Argon gas flow [l/min]	40	

From these experiments, HAZ were studied after a metallographic cross section. A parametric analyze in correlation with the HAZ dimensions, was carried out, in order to determine the significant processing parameters with respect to weld bead size. The second task was to optimized these parameters on a water quench Ti-6Al-4V plates, to study α' decomposition. Two LHT was then selected and applied in-situ, on Ti-6Al-4V weld with correct geometry. The main aim of this work was to softening the FZ weld, in order to improve the mechanical properties.

1. Results

3.1 Process window for Heat Treatment without fusion

The phase transformation solid→liquid observed at various laser parameters are illustrated on the power density-interaction time diagram (Figure 3). A process boundary between the Melting and No-Melting area has been highlighted. The upper limit of the boundary is (5.10^4 W.cm^{-2} ; 4.10^{-4}s), the lower limit (1.10^4 W.cm^{-2} ; 5.10^{-1} s).

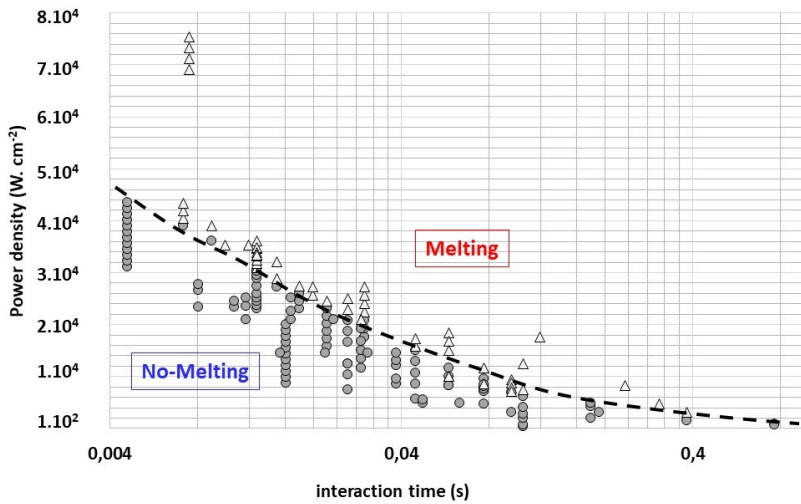


Figure 3: Investigation of the “heat treatment window” without fusion on Ti grade 2 thin sheet.

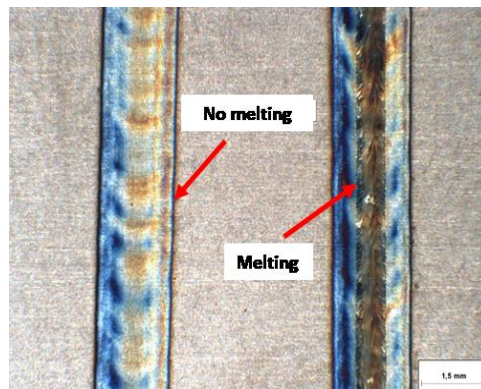


Figure 4: Example of laser track with Melting ($1,7 \cdot 10^4 \text{ W.cm}^{-2}$, $4,5 \cdot 10^2 \text{ s}$) or No-Melting ($1,3 \cdot 10^4 \text{ W.cm}^{-2}$, $4,5 \cdot 10^2 \text{ s}$) obtained after laser beam defocalisation.

The HAZ on plates are marked by the $\alpha \rightarrow \beta$ allotropic transformation. When the Ti CP grade 2 has been heated above the transus temperature T_β (887°C), the microstructural changes following the reaction $\alpha \rightarrow \beta$ and limits the outer edge of the HAZ. Beyond this frontier, no microstructural changes occur, and we have unaffected base metal [7].

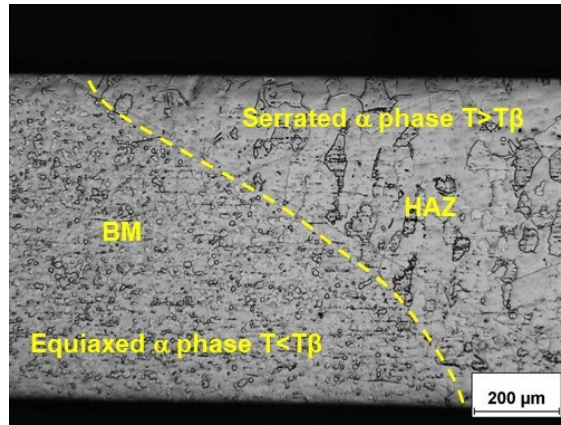


Figure 5: HAZ limit marked by the microstructural after $\alpha \rightarrow \beta$ transformation.

After determining a No-Melting domain for the LHT, the HAZ dimensions were determined by metallographic cross sections of the laser tracks. The microstructure was analyzed on the basis of the relationships between the process parameters and HAZ dimensions (Figure 6).

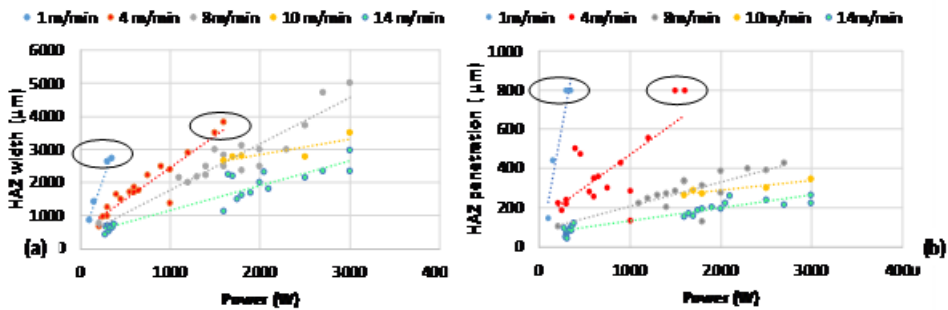


Figure 6: Variation of HAZ dimensions with the power and laser velocity (a) HAZ width, (b) HAZ depth.

It would be a great interest to determine a thermal cycle at which the martensite could be decomposed. In order to assess these process parameters on a martensitic microstructure, a set of parameters was carried out with a large and small defocusing distance, as a function of the incident power and laser velocity. The beam radius was adapted to scan a weld joint ranges from 1 mm to 2 mm. The selected parameters and their ranges are given in Table 3.

Table 3: Experimental parameters to optimize a LHT on a martensitic microstructure.

Power (W)	Number of level	Velocity (m.mm ⁻¹)	Defocusing (mm)	Beam radius (mm)
1500-1750	4	4	80	2

300-340	4	1	34	1
---------	---	---	----	---

Based on this experimental investigations, it can be conclude, from cross metallographic observations, that a local heating with a power of 1750 W, a velocity at 4 m.mm⁻¹ and a defocusing distance of 80 mm, has a sufficient effect to destabilize α' (Figure 7). On the other hand, for a diffusional transformation, with the formation of Widmanstätten microstructure, a power of 312 W, with a velocity at 1 m.mm⁻¹, a defocusing distance of 34 mm, seems to be necessary. The increase in hardness as observed for the two treated joints, is in agreement with previous work [5] [8]. It was attributed to the partial decomposition of α' to $\alpha+\beta$ after a stress relief-annealing treatment.

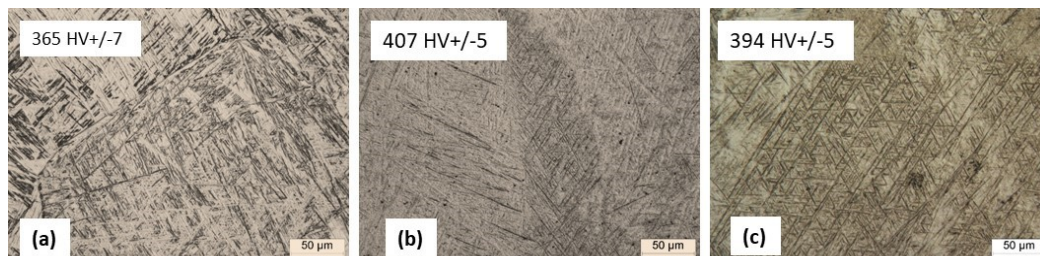


Figure 7: Effect of a LHT on a martensitic microstructure, (a) As water quenched, (b) α' destabilization for 1750 W, 1 m.mm⁻¹, 80 mm defocusing distance (700 J.cm⁻²), (c) Widmanstätten microstructure for 312 W, 4 m.mm⁻¹, 34 mm defocusing distance (1000 J.cm⁻²).

3.2 Application of LHT on welded joint after welding

For qualifying these two LHT cases, investigations were conducted on a butt joint, after laser welding (Table 4).

Table 4: Parameters for welding and Local Heat Treating.

Process	Power (W)	Velocity(m.mm ⁻¹)	Defocusing (mm)	Beam radius (mm)
Laser welding	1500	4,5	-0,3	0,16
LHT1	312	1	34	1
LHT2	1750	4	80	2

After a first laser scan, the LHT1 treatment showed no significant changes relative to the as-welded joint (Figure 8b). The microstructure consists of fine acicular α' in the FZ. Prior β grains are visible and similar than that seen in the as-welded joint, indicating that the thermal cycle does not produces temperature higher than T_{β} .

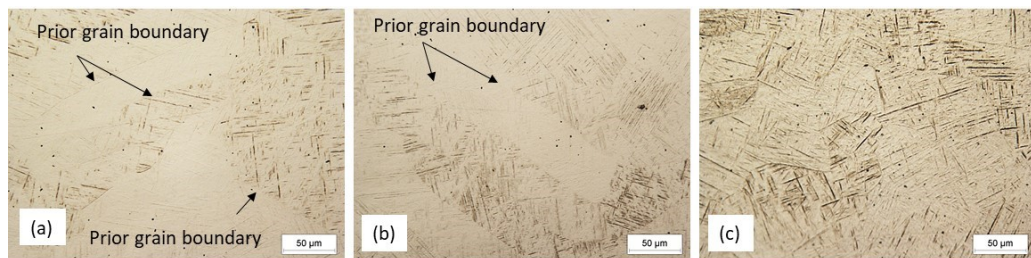


Figure 8: optical microstructure in FZ, (a) As-welded , (b) After one scan LHT1, (c) After one scan LHT2.

The hardness profile measured after the LHT1 treatment , is similar compared with the as-welded condition (Figure 9a).

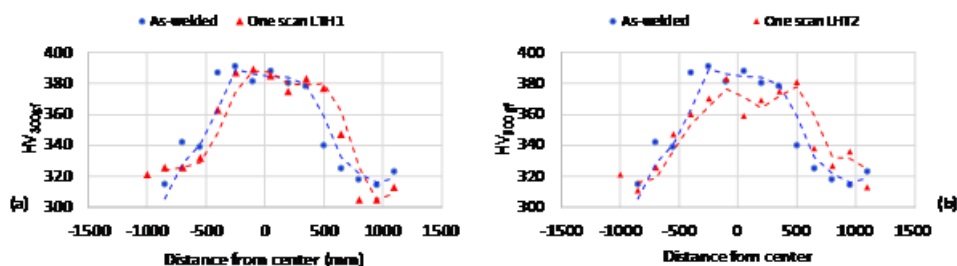


Figure 9: Hardness distribution in the FZ, (a) after one scan LHT1 treatment, (b) after one laser scan LHT2 treatment, compare to the as-welded joint.

On the other hand, for the LHT2 treatment, a metallurgical modification was clearly visible. The FZ is consisting of fine Widmanstätten microstructure which may be mostly martensitic (Figure 8c). As before, prior β grains remains unaltered compared to the as-welded. Therefore, we can notice a slight reduction for the hardness values in FZ, which could be associated to the partial martensite decomposition (Figure 9b). these values become more scattered in the one scan LHT2 than in the one scan LHT1 (Figure 9a).

Based on the optical micrographs, it can be seen that the microstructure in the FZ was not sufficiently coarsened after the LHT. The acicular morphology is still apparent. We can conclude that it is difficult to control both a sufficient temperature below the transus and enough dwelling time, to decompose α' and ensure the desired microstructure. As a consequence, the next stage of these investigations was to applied several laser scans to cumulate heating effects, in order to obtain a local softening in the FZ.

A second LHT treatment was then applied in the same conditions, after the heat treated joint had cooled, to avoid long heating times. Figure 10 shows the microstructure evolution after a second laser scan. The optical observations reveals a more pronounced α' decomposition, with a lath growth and α'/α interfaces more visible.

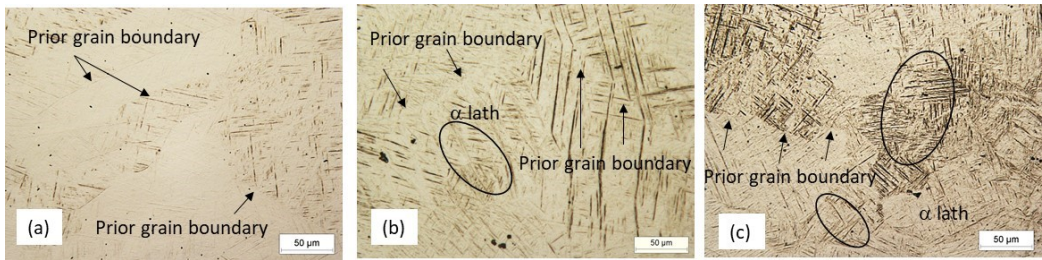


Figure 10: Microstructure in FZ, (a) As-welded , (b) After two scans LHT1, (c) After two scans LHT2.

The hardness value for the as-welded, LHT1 and LHT2 conditions, with one or two scan are shown in the Figure 11. The decrease in hardness seems to be consistent with the microstructure evolution, after the laser scanning. The cumulated tempering time from the second scan LHT1, seems to have a significant effect on the α' decomposition. The hardness distribution in FZ seems to be more homogeneous after a second LHT1 scan.

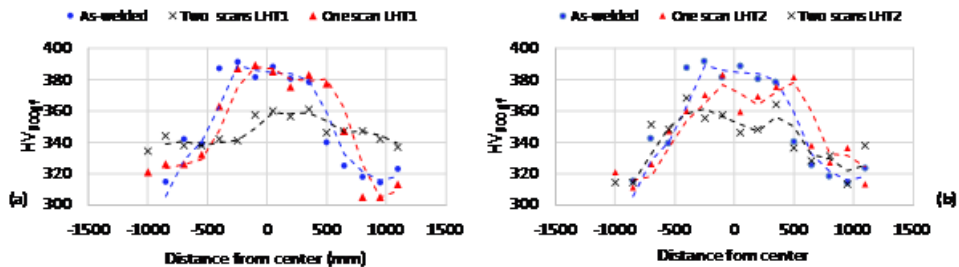


Figure 11: Hardness distribution in the FZ, (a) after two scans LHT1 treatment, (b) after two scans LHT2 treatment, compare to the as-welded joint.

1. Discussion

After one laser scan, the acicular microstructure and the remain prior β -grain, suggest the maximum temperature during LHT is below the beta-transus T_β [10]. The metallurgical effects of this treatment, is similar to a stress-relief annealing, which is consistent with previous work [4]. After a second laser scan, the α' decomposition takes place with a precipitation of fine α phase. The decrease of the hardness has been attributed to this precipitation. Nevertheless, it is difficult to distinguish between the α' and the α phases at microscopy scale.

The metallurgical changes in FZ after heat treatment depend on the initial microstructure, the reached maximum temperature and the cooling rate. Generally, heat treatments on Ti-6Al-4V weld joints, are carried out at a temperature below the β -transus to convert α' to a mixture of α and β phases [4] [7] [8]. A temperature above the β -transus favors coarsening of the final microstructure.

2. Conclusion

A local heat treatment seems to be suitable for heat treating martensitic microstructure for Ti-6Al-4V welded joints. The laser heating can decompose the α' martensite. The heat input and the treated area, are modulated by the following process parameters: power, velocity and beam diameter, varying with the defocused distance. In the case of insufficient α' decomposition, a laser

multi-scan can cumulate the microprecipitation effects for softening Ti-6Al-4V welds. Future work will focus on the mechanical properties as a function of minimum number of laser scan to obtain desired microstructure.

3. Acknowledgements

The authors wish to express their gratitude to J. Pecune for his valuable technical support.

4. References

5. [1] X. Cao, M. Jahazi, *Opt. and lasers Eng.* 47 (2009) 1231-1241.
- [2] A. Squillace, H. Prisco, *J. Mat. Proc. Tech.* 212 (2012) 427-436.
- [3] C. Kumar, M. Das, *Opt. and lasers Eng.* 95 (2017) 52-58.
- [4] H.K Abu-Syed, X. Cao, *Met and Mat. Trans.* 43 (1996) 4171-4184.
- [5] T. Ahmed, H. J. Rack, *Mat. Sci. Eng.* 243 (1998) 206-2011.
- [6] J.D Béguin, V. Gazagne, *Mat. Sc. For.* 941 (2018) 845-850.
- [7] S. Lathabai, B.L Jarvis, *Mat. Sci. Eng.* 299 (2001) 81-93.
- [8] X.Y Zhang, G. Fang, *J. Alloys and comp.* 735 (2018) 1562-1575.
- [9] F.X Gil, D. Rodriguez, *J. of Alloys and comp.* 234 (1996) 287-289.
- [10] M.J. Hu, J.H. Liu, *Mat. Sci. Eng.* 19 (2009) 324-329.